JPEDAV (2007) 28:258–264
DOI: 10.1007/s11669-007-9021-1
1547-7037 ©ASM International

Modeling of Plate-Like Precipitates in Aluminum Alloys—Comparison between Phase Field and Cellular Automaton Methods

W. Wang, J. L. Murray, S. Y. Hu, L. Q. Chen and H. Weiland

(Submitted April 7, 2006)

This report compares two approaches for simulating microstructure evolution of plate-like precipitates during artificial ageing of aluminum alloys: the phase field and the cellular automaton methods. Although both methods are based on thermodynamics, they handle the kinetics in quite different ways, each with its own advantages and disadvantages. Both methods were applied to the growth of semi-coherent plate-like θ′ precipitates in Al-4 wt% Cu. Good agreement is found between the results of these two models, as well as experiments. A combination of these two methods would provide a novel approach that is both physically sound and computationally effective for the application of precipitation modeling.

Keywords Aluminum alloys, Cellular automation, Ledge growth, Phase field, Precipitation

1. Introduction

The objective of this work was to build an ageing tool to predict the microstructural evolution of precipitates during artificial ageing of heat-treatable aluminum alloys. In the present stage of the project, we focus on simulating precipitation of semi-coherent strengthening phases like θ′ in Al-Cu, which usually has a plate-like morphology.[1] A key feature of the microstructure is the high aspect ratio of the plates.[2,3] Most researchers[3-5] attribute the high aspect ratio of θ′ to different lengthening and thickening kinetics. The physical mechanism for plate thickening is the motion of ledges across the broad face. Thus a major challenge encountered in developing a precipitation model is how to incorporate the ledge mechanism into the algorithm.

Many researchers have done a lot of work on investigating ledge mechanism. Figure 1 is a two-dimensional graphic illustration of a plate-like precipitate with its broad surface composed of stepwise ledges. The ledges have a uniform height h and are evenly distributed at a spacing s. If all the ledges have an instantaneous velocity along the step surface, v_s, the overall growth velocity of the interface normal to the step surface (or the thickening rate of the precipitate), v_H, is

$$v_H = v_s h/s. \quad \text{(Eq 1)}$$

Jones and Trivedi[6,7] related the growth rate of ledge with supersaturation

$$\Omega = 2\mathrm{Pe}\alpha(\mathrm{Pe}), \quad \text{(Eq 2)}$$

where Pe is a dimensionless Péclet number, defined as $\mathrm{Pe} = v_s h/(2D)$, where D is the diffusivity of solute in the matrix. The function α was evaluated numerically by Jones and Trivedi. Later Atkinson[8] obtained a mathematical solution for this function. And this solution was verified by other researchers using a finite difference model to directly simulate ledge growth.[9,10]

Equation 1 indicates that both the ledge velocity and the ledge spacing can affect the precipitate thickening rate, and Eq 2 relates the ledge velocity to the supersaturation. Aaronson et al.[3,11] assumed that during the early stage of precipitation the supersaturation does not change and the ledge spacing is almost constant, thus the thickness of the precipitate increases linearly with the time. However, such an assumption is no longer appropriate at the later stage of precipitation, because of the strong interaction between ledges. Doherty et al.[2,5,12] argued that if the critical diffusion length is much larger than the ledge spacing, almost all the solute atoms that diffuse to the broad surface of the precipitate can be caught by one of the ledges, and the thickness of the precipitate has a nearly parabolic dependence on ageing time.

The approach taken in this work is to build a computational model-based thermodynamics of phase transformation. We tried two types of modeling methods—the phase field and cellular automaton methods—both of which are widely utilized by academic researchers in study of other phase transformation problems.[13] Although both models are based on thermodynamics, they handle the kinetics of phase transformation in quite different ways. The algorithms of both models are reviewed briefly in the following sections. And both were applied to simulate ledge growth in θ′ precipitation in Al-4wt% Cu. We compared the results of

W. Wang, J. L. Murray, and **H. Weiland,** Alcoa Technical Center, 100 Technical Drive, Alcoa Center 15069 PA, USA. **S. Y. Hu,** and **L. Q. Chen,** Department of Material Science and Engineering, Penn State University, University Park 16802 PA, USA. Contact e-mail: wei.wang@alcoa.com

these two models in search of a method suitable for modeling precipitation in aluminum alloys.

2. Modeling Approach

2.1 Phase Field Model

Recently, Chen and co-workers[14-16] have developed a phase field model for precipitation in aluminum alloys. The phase field method has been widely used for liquid-solid transformations,[13] but its application in precipitation is still relatively new. The modeling approach will be briefly reviewed in this paper in the following section, and the reader is advised to refer to the work of Hu[16] for more details.

The phase field model uses an order parameter (ϕ) to differentiate the matrix and precipitate phases. The order parameter has a constant value inside each phase region and changes smoothly in the phase boundary layer. The growth rate of the precipitate is related to the rate of change of the order parameter, which can be obtained by solving the following two coupled equations

$$\dot{\phi} = M[\varepsilon^2\nabla^2\phi - \partial G/\partial\phi] \quad \text{(Eq 3)}$$

$$\dot{C} = \nabla[(D/G_{CC})\nabla(\partial G/\partial C)] \quad \text{(Eq 4)}$$

where C is composition, D diffusivity, M mobility coefficient for the order parameter, ε a coefficient related to the interfacial energy, and G is the Gibbs free energy, which is a function of both ϕ and C (G_{CC} stands for $\partial^2 G/\partial C^2$). The coefficient M is an adjustable factor in the model because of the lack of a way to directly measure the physical mobility of the matrix-precipitate interface.

It has been proved that the phase field model can provide good qualitative predictions of the growth behavior of θ' precipitate in Al-Cu alloys,[14-16] but it needs further improvement to provide the quantitative simulations that are required for industrial applications. Therefore, it is necessary to fine-tune the mobility coefficient (M). As mentioned above, it is not possible to carry out a direct comparison with experiment. An alternative is to correlate the mobility coefficient with some other experimentally measurable quantity.

2.2 Cellular Automaton Model

The kinetics of ledge growth is simulated by a cellular automaton model which is based on the model originally developed by Wang and their co-workers[17,18] for solidification in nickel-based superalloys. This model has been modified to be applicable to solid-state precipitation in aluminum alloys. A two-dimensional schematic illustration of the model configuration is given in Fig. 2. The simulation domain ABCD is divided into uniform square cells: the blank cells represent matrix phase, the fully filled cells represent the precipitate phase, and the partially filled cells represent the interface containing stepwise ledges. The matrix-precipitate boundary is highlighted by line EFGH.

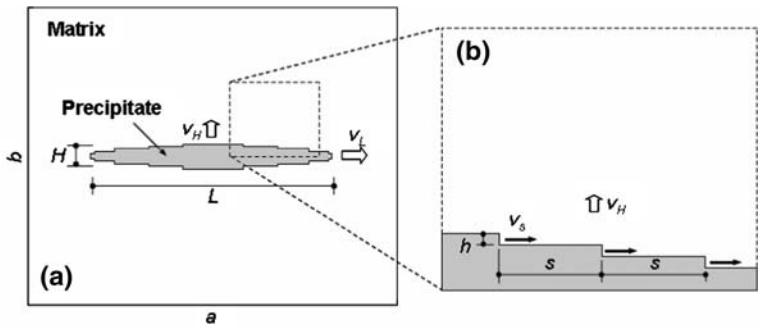

Fig. 1 (**a**) A 2D schematic illustration of a plate-like precipitate. (**b**) Magnification of the broad surface of the precipitate composed of stepwise ledges.

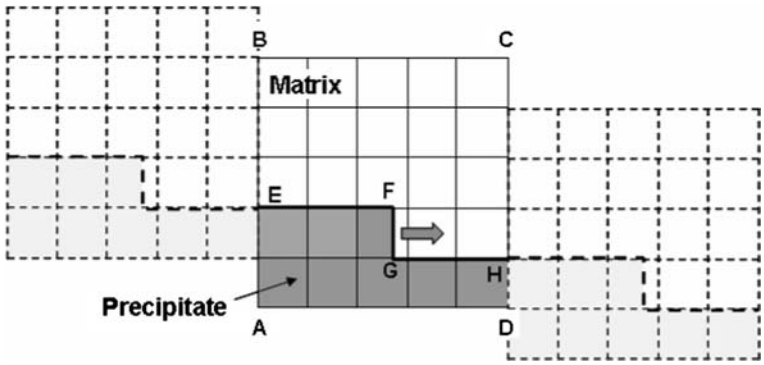

Fig. 2 A schematic illustration of the cellular automaton model configuration.

The plate can thicken in two ways: (1) the ledge can move towards the right when the cell adjacent to FG transforms from matrix to precipitate, without any increase of the total interfacial area or (2) a new ledge can nucleate, increasing both the amount of precipitate and the total interfacial area. That is, thickening by ledge nucleation requires extra activation energy. Only the ledge growth algorithm has been incorporated in the current model; and the ledge nucleation algorithm will be incorporated into the model in the future. When a ledge migrates to the edge of a plate-like precipitate, it blends into the incoherent edge, and the number of ledges on the broad surface decreases by one, which will then affect the average ledge spacing. In the current model, it is assumed that there are always enough new ledges nucleated to compensate the loss of ledges at plate edge, and the ledge spacing remains constant.

The migration rate of the ledge FG is determined by the flux across the step. A finite difference method is incorporated in the model to solve diffusion in the matrix, and the composition at the step in the matrix is calculated from the phase diagram using ThermoCalc software. Two types of boundary condition can be applied to the edges of the domain: closed boundary condition and periodic boundary condition. When the closed boundary condition is applied, the flux across the edge of the domain is set to zero. The periodic boundary condition can only be applied to the left and right edges of the domain AB and CD. The periodic boundary condition can be visualized by ''copying and pasting'' the domain ABCD to its left and right sides, but shifted upward or downward by a distance equal to the ledge height, as illustrated in Fig. 2. In this way, the original one-ledge configuration becomes a train of ledges, with a ledge spacing equal to the width of the domain. When the ledge FG moves to the right edge (CD), it does not disappear there but re-enters the domain at the left edge (AB).

Because it incorporates sharp interfaces and discontinuous ledges, the cellular automaton model can be used to relate the precipitate thickening rate with the ledge spacing, which is an experimentally measurable quantity. If the phase field model can be correlated with the cellular automaton model, then the model parameter (M) can be quantitatively evaluated against experiments.

3. Simulation Results

We now have two models for precipitation; the simulation results of each model are presented in this section, followed by comparison between them.

3.1 Phase Field Results

If one is interested only in the thickening behavior of the plate, then one-dimensional simulations can provide good results, because the plates usually have high aspect ratio. The model configuration is illustrated in Fig. 3(a), and the parameters are listed in Table 1. The interface is initially located at the left end of the domain and moves to the right. A set of nine simulations was performed, in which the mobility coefficient (M) varied from 1×10^{-9} to 1×10^{-5} (1/s)/(J/mol), resulting in different growth velocities of the interface. The volume fraction of the precipitate is the size of the precipitate divided by the length of the domain. The simulation results are given in Fig. 3(b).

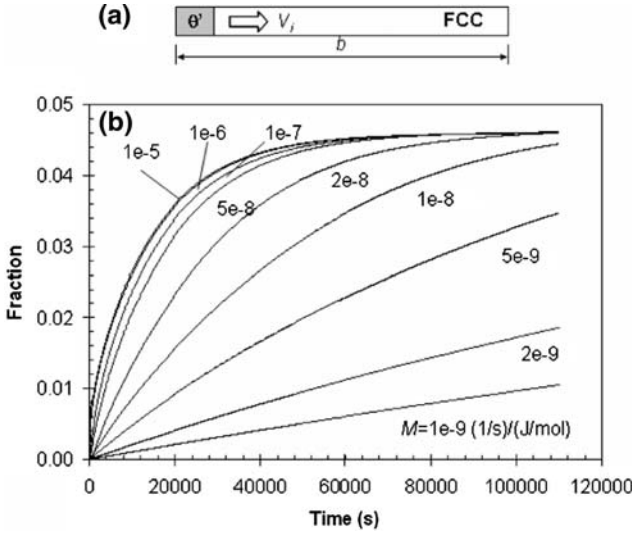

Fig. 3 (**a**) 1D phase field simulation configuration. (**b**) Increase of the precipitate fraction against time with different mobility coefficients (M).

Table 1 Parameters for phase field simulations

Parameter	Symbol	Value	Unit
Alloy system	Al-Cu	-	-
Initial composition	C_0	1.74 (4)	at% (wt%)
Temperature	T	498 (225)	K (°C)
Diffusivity	D	5.09×10^{-19}	m^2/s
Precipitate composition	C_P	32.8	at%
Equilibrium composition at the interface in the matrix	C_S	0.25	at%
Mobility coefficient	M	1×10^{-9}-1×10^{-5}	(1/s)/(J/mol)
Cell size	Δx	1.2	nm
Time step	Δt	$(\Delta x)^2/(10D)$	-

Figure 3(b) shows that the mobility coefficient (M) does have a significant effect on the precipitate thickening behavior. When the value of M is in the low range the fraction of precipitate increases almost linearly with time, but as M increases this linear thickening behavior gradually transforms into a roughly parabolic one and finally approaches an upper limit. This upper limit corresponds to diffusion-controlled growth where the thickening behavior is independent of the interface mobility parameter (M).

3.2 Cellular Automaton Results

The cellular automaton model is first validated against Atkinson's[8] analytical solution and then applied to simulate precipitate thickening. The alloy system, initial composition, diffusivity and cell size are the same as were previously used in the phase field simulations (see Table 1), but the simulations are carried out in two dimensions. The simulation domain

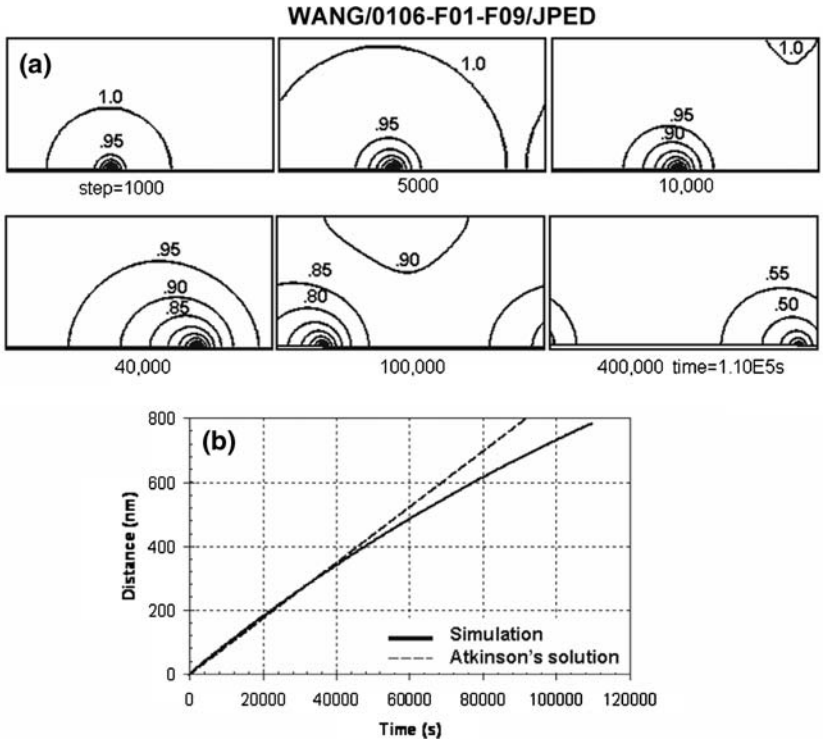

Fig. 4 (**a**) Simulation results of a single ledge in a domain with periodic boundary condition. (**b**) The ledge displacement against time.

contains 256×128 unit cells, and the closed boundary condition is applied to the upper and lower edges of the domain while the periodic boundary condition is applied to the left and right edges. Only one ledge is introduced at the matrix-precipitate interface and its height is equal to one cell size. The simulation results are presented in Fig. 4.

Figure 4(a) shows six snapshots, from various simulation times, of the contour lines of dimensionless composition, defined as $\Gamma = (C - C_S)/(C_0 - C_S)$. The contour lines are dense around the moving ledge, indicating a high local composition gradient. The solute distribution is asymmetric around the ledge, and the gradient is higher in front of the ledge than behind it. Because of the periodic boundary condition, as the ledge migrates to the edge of the domain (see the result at 40,000 time steps) it does not vanish there but re-enters the domain from the opposite side (see the result at 100,000 steps). The displacement of the ledge is plotted against the simulation time in Fig. 4(b), and Atkinson's[8] analytical solution is also plotted for comparison. The cellular automaton prediction shows excellent correlation with Atkinson's solution in the early stage of ledge growth, but shows obvious deviation at later times. This is because Atkinson's analysis assumes the overall composition in the matrix does not change, but in the cellular automaton simulations the matrix composition decreases as the ledge grows, which is closer to reality.

In the simulation shown in Fig. 4, although there is only one ledge present in the domain, it must be understood as a train of ledges with a uniform spacing equal to the width of the domain due to the periodic boundary condition. In the following simulations a two-ledge configuration is adopted to more clearly illustrate how ledges interact. As shown in Fig. 5(a), the rectangular domain (composed of 256×128 unit cells) contains a phase boundary with two ledges moving in the same direction. The height of both ledges is equal to the cell size ($h = \Delta x$), and they are separated by a distance equal to half of the width of the domain ($s = 128\Delta x$). A dimensionless parameter m is defined as the normalized ledge spacing over the ledge height, $m = s/h$. Figure 5(a) shows the simulation results at 1000, 10,000, and 100,000 time steps. The two ledges always move at the same rate because of the identical diffusion patterns. At the beginning of the simulation these two ledges grow independently, as shown in the result at 1000 steps, and the two $\Gamma = 1$ contours associated with each ledge have not contacted yet. As the ledges continue to grow, the diffusion fields start to overlap, and this affects the growth rate of both ledges. After 100,000 steps, the interaction between these two ledges has totally changed the diffusion pattern far away from the ledges, but has less effect on the short-range diffusion pattern around the ledges.

Three more examples with different ledge spacings, $m = 64$, 32, and 16, are shown in Fig. 5(b), (c), and (d), respectively. A general trend in these results is that the interaction between the diffusion fields of the ledges becomes more significant as the ledge spacing decreases. A distinctive transition is observed in the diffusion fields: approximately circular contours around the ledges and almost flat lines parallel with the interface away from the ledges, and this transition occurs at a distance that is a little less than half of the ledge spacing away from the interface. In the case of $m = 16$, this distance is almost negligible compared with the height of the domain, and the diffusion pattern is characterized by the long range unidirectional diffusion towards the interface.

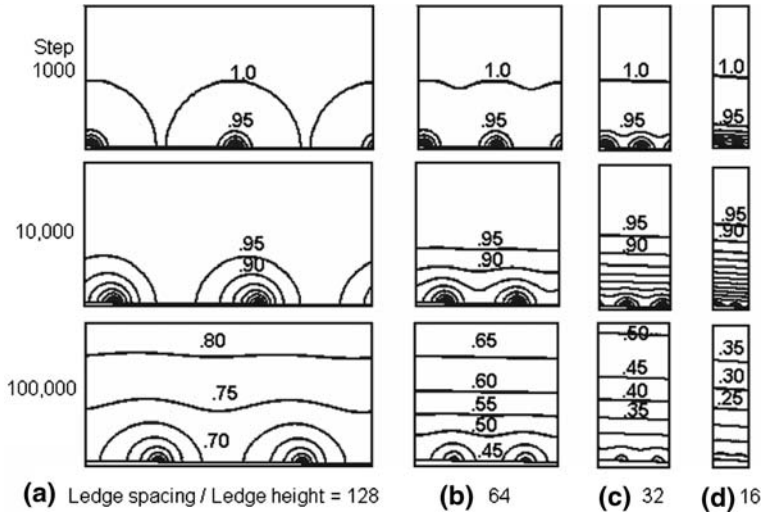

Fig. 5 Simulation results of two-ledge growth in a domain with periodic boundary condition.

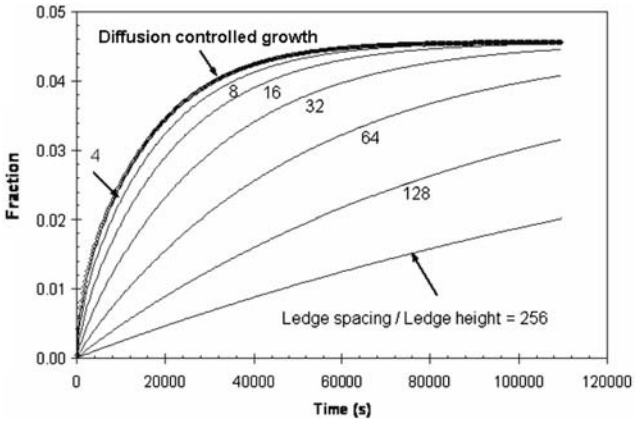

Fig. 6 Relationship between the precipitate fraction and time with different spacings.

In the simulations shown in Fig. 5, the volume fraction of the precipitate phase is calculated as the area of the precipitate over the total area of the domain. The increases in the precipitate fraction with time are plotted in Fig. 6. The phase field result for diffusion-controlled growth ($M = 1\times10^{-5}$ (1/s)/(J/mol)) is also plotted in this figure for comparison. An obvious trend is that as the ledge spacing decreases, the relationship between the phase fraction and time shifts from a low-slope straight line to a concave curve and finally approaches the diffusion-controlled-growth limit.

4. Discussion

4.1 Model Comparison

The results of the cellular automaton model in Fig. 6 exhibit an obvious resemblance to those of the phase field model in Fig. 3. A one-to-one comparison between these results is illustrated in Fig. 7. As shown in Fig. 7(a), both the cellular automaton model ($m = 256$) and the phase field model ($M = 1\text{-}3\times10^{-9}$ (1/s)/(J/mol)) predict an approximately linear relationship between the precipitate fraction and time. In the phase field simulations the average thickening rate (the mean slope of the fraction-time curve) is roughly proportional to the mobility coefficient M. The cellular automaton result with $m = 256$ almost exactly coincides with the phase field model prediction with $M = 2.3\times10^{-9}$. But such a good match is not found in Fig. 7(b), where the cellular automaton result ($m = 128$) initially follows the phase field prediction ($M = 5\times10^{-9}$) but gradually drops below it and crosses the $M = 4.5\times10^{-9}$ curve. In Fig. 7(c) the cellular automaton result ($m = 32$) intercepts several curves of the phase field model with $M = 1 - 3\times10^{-8}$. A good correlation is found again in Fig. 7(d) where both the cellular automaton ($m = 8$) and the phase field ($M = 6\times10^{-8}\text{-}1\times10^{-7}$) predictions approach the diffusion-controlled-growth limit.

Thus a general correlation is found between the phase field and cellular automaton models, although with some deviations for ledge spacing on the order of ledge height. Figure 8 shows the relationship between the normalized ledge spacing (m) in the cellular automaton model and the mobility coefficient (M) in the phase field model. An inversely proportional relationship, MP $1/m$, seems to be a good correlation on condition that the ledge spacing is much larger than the ledge height ($m \geq 8$).

4.2 Verification against Experiments

The model comparison indicates an inverse correlation between the mobility coefficient (M) in the phase field model and the normalized ledge spacing (m) in the cellular automaton model. The experimentally measured ledge spacing is in the range of 150-300 nm for θ' plate in Al-4wt%Cu alloy during the precipitate growth stage.[11,19] The measurement of ledge spacing requires the precipitate to have a certain size and thickness, thus no data is available in the early period of precipitation. The ledge height is determined by the lattice parameters of the matrix and precipitate,[4] and is taken as

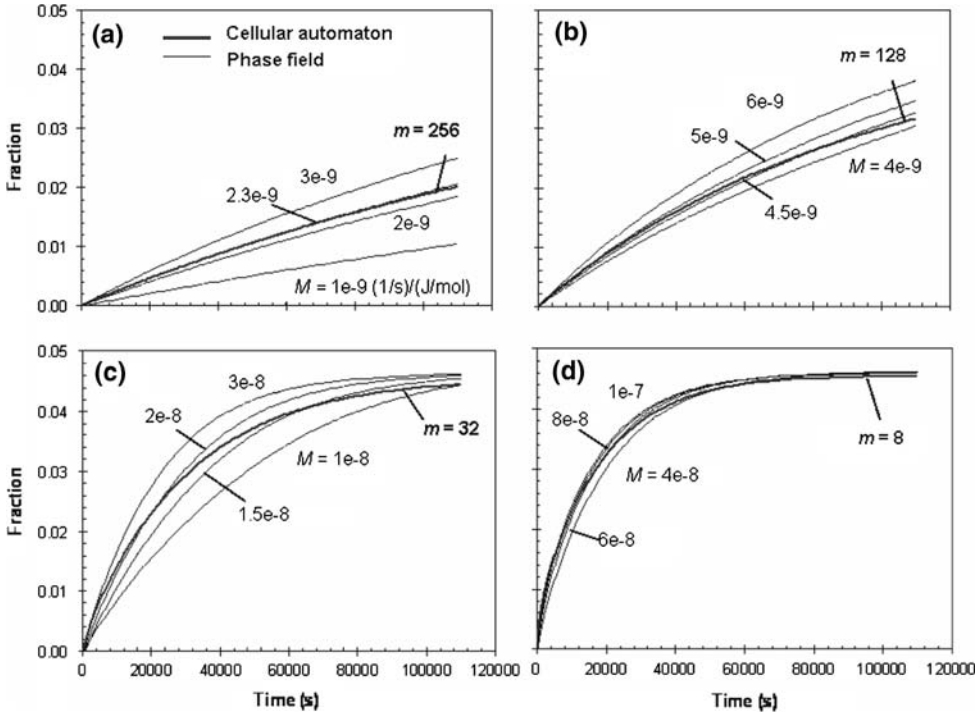

Fig. 7 Comparison between the cellular automaton and the phase field results.

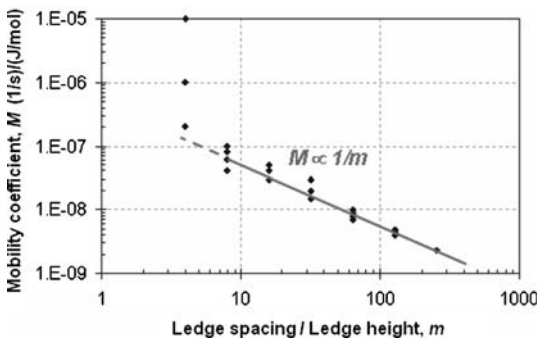

Fig. 8 Correlation between the mobility coefficient (M) in the phase field model and the normalized ledge spacing (m) is the cellular automaton model.

1.2 nm in all the simulations. Thus for this system, the normalized ledge spacing in the cellular automaton model is about m = 128-256, and the corresponding mobility coefficient in the phase field model is $M = 2.3\text{-}4.5 \times 10^{-9}$ (1/s)/(J/mol).

Figure 9 shows the results of both models with the evaluated parameters. The vertical coordinate represents half thickness of the precipitate and the horizontal coordinate represents ageing time. The initial half thickness of the precipitate is 1.2 nm, equal to the ledge height. The solid lines are cellular automaton results and the dash lines are the phase field predictions. Also plotted in this figure are the experimental data by Merle and Fouquet.[20] It is noticed that those experimental data are initially close to the m = 64 curve and then fall into the expected range marked by the curves m = 128 and 256. This deviation occurs at the initial time period less than 7 h when the half thickness of the precipitate does not exceed 3.6 nm. This suggests that the ledge spacing is between 75 and 150 nm during the initial growth of precipitate and then increases to the range of 150-300 nm. The increase of ledge spacing with time, or decrease of number density of ledges with time, could be due to the expectation that the nucleation of ledges becomes more difficult as solute supersaturation decreases with time. It is hoped that we could match our simulations better with experimental results by incorporating ledge nucleation algorithm into the model.

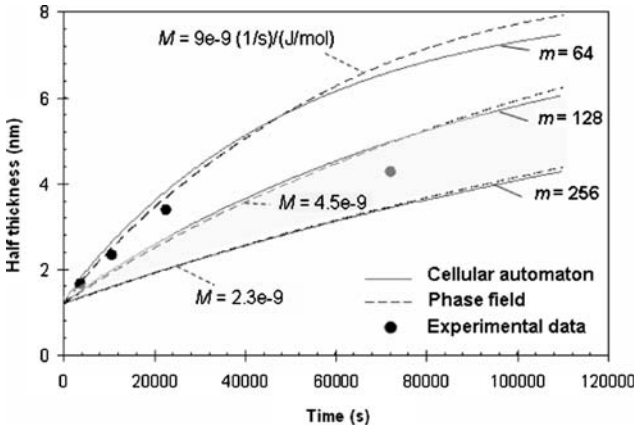

Fig. 9 Comparison between the model predictions with experiments.

5. Summary

We have taken two approaches—phase field and cellular automaton methods—to model precipitation in aluminum alloys. Both models are constructed based on thermodynamics, but they handle the kinetics in different ways. With the introduction of the interfacial mobility coefficient the phase field model can reproduce different growth kinetics, from diffusion-controlled growth to mobility controlled growth. Unlike the phase field model that defines a diffuse phase boundary layer, the cellular automaton model adopts a sharp interface definition, which allows it to directly simulate the growth of individual ledges.

Both models have been verified against previous analytical solutions and experiments. Precipitation of θ' phase in a binary Al-4wt%Cu alloy was chosen as the benchmarking example, and good agreement was found between the model predictions and experiments. A combination of these two methods would provide a novel approach that is both physically sound and computationally effective for the application of precipitation modeling.

Acknowledgements

The authors would like to acknowledge valuable conversations with Prof. Roger Doherty of Drexel University and Ralph T. Shuey of Alcoa Technical Center.

References

1. H.I. Aaronson and C. Laird, Structure and Migration Kinetics of Alpha: Theta Prime Boundaries in Al-4 Pct Cu: Part I-Interfacial Structures, *Trans. Metall. Soc. AIME*, 1968, **242**, p 1393-1403
2. Y.H. Chen and R.D. Doherty, On the Growth Kinetics of Plate-Shaped Precipitates in Aluminum-Copper and Aluminum-Gold Alloys, *Scripta Metall.*, 1977, **11**, p 725-729
3. H.I. Aaronson and C. Laird, Structure and Migration Kinetics of Alpha: Theta Prime Boundaries in Al-4 Pct Cu: Part II-Kinetics of Growth, *Trans. Metall. Soc. AIME*, 1968, **242**, p 1437-1448
4. U. Dahmen and K.H. Westmacott, Ledge Structure and the Mechanism of Theta Prime Precipitate Growth in Al-Cu, *Phys. Stat. Sol.*, 1983, **80**, p 249-262
5. R.D. Doherty, Diffusive phase transformations in the solid state, in *Physical Metallurgy*, R.W. Cahn and P. Haasen, eds. Elsevier Science B.V., Norther-Holland, 1996, p 1363-1505
6. G.J. Jones and R.K. Trivedi, Lateral Growth in Solid-Solid Phase Transformations, *J. Appl. Phys.*, 1971, **42**, p 4299-4304
7. G.J. Jones and R.K. Trivedi, The Kinetics of Lateral Growth, *J. Cryst. Growth*, 1975, **29**, p 155-166
8. C. Atkinson, The Growth Kinetics of Individual Ledges during Solid-Solid Phase Transformations. *Proc. Roy. Soc. Lond.*, 1981, **A378**, p 351-368
9. R.D. Doherty and B. Cantor, *Computer Modelling of Ledge Growth Kinetics. in Solid to Solid Phase Transformations*, 10-14 Aug 1981. The Metallurgical Society/AIME, Warrendale, Pittsburgh, PA, 1981, p 547
10. M. Enomoto, Computer Modeling of the Growth Kinetics of Ledged Interphase Boundaries - I. Single Step and Infinite Train of Steps, *Acta Metall.*, 1987, **35**, p 935-945
11. R. Sankaran and C. Laird, Kinetics of Growth of Platelike Precipitates, *Acta Metall.*, 1974, **22**, p 957-969
12. R.D. Doherty, M. Ferrante, and Y.H. Chen, Reply to Discussions on "The Growth Kinetics of Plate-Shaped Precipitates", *Scripta Metall.*, 1977, **11**, p 733-739
13. W.J. Boettinger, S.R. Coriell, A.L. Greer, A. Karma, W. Kurz, M. Rappaz, and R. Trivedi, Solidification Microstructures: Recent Developments, Future Directions, *Acta Mater.*, 2000, **48**, p 43-70
14. D.Y. Li and L.Q. Chen, Computer Simulation of Stress-Oriented Nucleation and Growth of Theta Prime Precipitates in Al-Cu Alloys, *Acta Mater.*, 1998, **46**(8), p 2573-2585
15. V. Vaithyanathan, C. Wolverton, and L.Q. Chen, Multiscale Modeling of Theta Prime Precipitation in Al-Cu Binary Alloys, *Acta Mater.*, 2004, **52**, p 2973-2987
16. S.Y. Hu, Phase-Field Models of Microstructure Evolution in a System with Elastic Inhomogeneity and Defects, in Department of Materials Science and Engineering. PhD Thesis, Pennsylvania State University, State College, 2004
17. W. Wang, A Mathematical Model of Dendritic Microstructures in Nickel-Based Superalloys, in Department of Materials. PhD Thesis, Imperial College London, London, 2003
18. W. Wang, P.D. Lee, and M. McLean, A Model of Solidification Microstructures in Nickel Based Superalloys: Predicting Primary Dendrite Spacing Selection, *Acta Mater.*, 2003, **51**, p 2971-2987
19. S. Elangovan and M.R. Plichta, Measurement of the Interledge Spacing on Theta Prime Precipitates in Al-Cu Alloys, *Scripta Metall.*, 1986, **20**, p 575-580
20. P. Merle and F. Fouquet, Coarsening of Theta Prime Plates in Al-Cu Alloys-I Experimental Determination of Mechanisms, *Acta Metall.*, 1981, **29**, p 1919-1927